

The Double-Channel Contact Recombination and Separation of Geminate Radical Ion Pairs in a Coulomb Well

Anatoly I. Ivanov*

Department of Physics, Volgograd State University, University Avenue, 100, Volgograd 400062, Russia

Anatoly I. Burshtein†

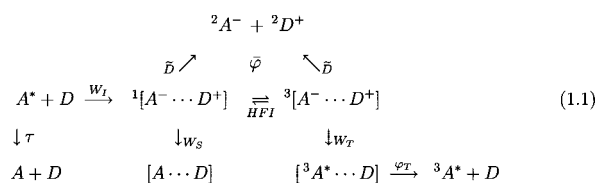
Weizmann Institute of Science, Rehovot 76100, Israel

Received: January 1, 2008; Revised Manuscript Received: February 27, 2008

The influence of the Coulomb attraction on photogenerated singlet radical ion pairs' separation and their geminate recombination to singlet and triplet neutral products is considered. Making use of the contact approximation and the rate or Hamiltonian description of the spin conversion, the quantum yields of recombination products and their diffusional dependence are investigated and fitted to the available experimental data. The nonmonotonous behavior of the triplet quantum yield of neutral products on both the Onsager radius and the triplet charge recombination rate constant are revealed and discussed in detail.

I. Introduction

The bimolecular fluorescence quenching by electron transfer, producing the radical ion pair (RIP) in the same spin state as its precursor, initiates a number of chemical transformations. The simplest among them are the geminate recombination and the radical ion separation. In actuality, it appears that even these processes are governed by a rather complex mechanism. For example, RIPs created in their singlet state may transform into a triplet state and recombine in both the singlet and triplet states of the neutral products. The triplet products of the geminate recombination of singlet-born RIPs were detected and discussed repeatedly.^{1–10} These explorations have led to the following scheme showing the possible transformations in the RIP and their sequence.



Here the singlet, doublet, and triplet states are indicated by left-hand superscripts 1, 2, and 3, respectively. W_I and W_S , W_T are the rates of the charge separation and the charge recombination to the singlet and triplet states of the products, correspondingly. The $\bar{\varphi}$ is the quantum yield of RIP separation, and φ_T is the yield of the excited triplet product of their recombination. \bar{D} is the encounter diffusion coefficient, being equal to the sum of the diffusion coefficients of A^- and D^+ . The quantum yield of the free ions, A^- and D^+ , is $\phi = (1 - \eta)\bar{\varphi}$, where η is the yield of A^* fluorescence.

Specifically, the scenario (1.1) is realized in the systems consisting of the excited perylene (A, electron acceptor) and N, N' -dimethylaniline (D, electron donor). Using the dimethyl sulfoxide–glycerol mixtures as the solvent, the reaction kinetics

in this system have been studied for a wide variation of viscosities, keeping all solvent parameters constant, except for the encounter diffusion coefficient.^{11–13} These experiments have revealed the nontrivial dependence of the quantum yields of the free ions as well as the singlet and the triplet neutral products of their recombination on the solvent viscosity. Although, to our knowledge, it is the only measurement of such a dependence, its qualitative behavior might be expected to be universal at least in the area of slow diffusion.

At first, the experimental data for recombination and ionization were fitted with the simplest model, including two rather rough approximations: (i) the rate (incoherent) model of spin conversion and (ii) the contact charge recombination.¹³ Later, these weaknesses were surmounted. In the framework of the incoherent spin conversion model, it was shown that the experimental data for recombination and ionization can be satisfactory fitted only with the noncontact ionization, provided that the recombination is also noncontact and even more distant than ionization.^{14,15} Recently, the incoherent model of spin conversion was substituted with a true hyperfine interaction (HFI) mechanism of coherent spin conversion.^{16,17}

These investigations have demonstrated that the quantum yields of the geminate RIP recombination to the singlet and triplet products can be well fitted to the available experimental data only with the value of the effective HFI constant, A , which is 20 times as large as that found from the experimentally determined HFI constants of the ion radicals participating in the reaction.¹⁷ Such a huge discrepancy calls for a revision of the model. The analytical solution obtained in ref 16 shows the magnitude of the quantum yields, φ_S and φ_T , to depend on the value of A , only through the dimensionless parameter $A\tau_d$, where $\tau_d = \sigma^2/\bar{D}$ is the encounter time of the neutral particles. Apparently, the value of $A\tau_d$ does not change if A reduces but τ_d increases accordingly. This may indicate that the reason for the overestimation of A is due to underestimation of the encounter time resulting from neglecting an important factor: the Coulomb interaction between the counterions. Indeed, the Coulomb attraction increases the lifetime of the nonreactive RIP by the factor¹⁸

* To whom correspondence should be addressed. E-mail: physic@vlink.ru.

† E-mail: Cfbursh@wisemail.weizmann.ac.il.

$$\frac{\tau_c}{\tau_d} = \frac{\sigma}{r_c} [e^{r_c/\sigma} - 1] \quad (1.2)$$

where τ_c is the encounter time accounting for the Coulomb attraction, $r_c = e^2/(\epsilon k_B T)$ is the Onsager radius, ϵ is the static dielectric permittivity of the solvent, k_B is the Boltzmann constant, and T is the temperature. For the dimethyl sulfoxide–glycerol mixtures, the static dielectric permittivity is $\epsilon \approx 43$, and we obtain $r_c \approx 12 \text{ \AA}$ at room temperature. This increases the encounter time by a factor of 2.5. It should be emphasized that this estimation is very rough, but it shows that the Coulomb attraction prolonging the pair lifetime can reduce the HFI constant needed for the fitting. However, this estimation, taking into account the diffusional decay of the geminate pair, totally ignores the influence of the reaction on the lifetime. For the reacting particles, one more channel of the geminate pair decay appears. It is well-known that the particles during the encounter time can experience a lot of collisions at contact distance. Obviously, if the particles can react at such contacts, the pairs can disappear before their diffusional decay. In other words, the reaction shortens the lifetime of the geminate pair.¹⁸ Moreover, the interior attraction affects the effectiveness of the recombination, shortening the time span between the contacts. These reasonings show that there is a multiplicity of interdependent mechanisms for the Coulomb interaction, impacting on the RIP recombination and separation kinetics. To answer the question regarding the extent of the Coulomb attraction's influence on the fitting parameters, a model incorporating all of these mechanisms should be explored.

In this paper, we show how the Coulomb attraction changes the previous results and allows to get reasonable values for the HFI constant from the best fit.

II. Coherent Spin Conversion Assistance of Double-Channel Geminate Recombination

The coherent evolution of an ensemble of RIPs with respect to spin and space degrees of freedom is described in terms of the distance-dependent spin density matrix $\hat{m}(r, t)$.^{16,19,20}

$$\frac{\partial \hat{m}(r, t)}{\partial t} = \hat{L}_c \hat{m}(r, t) - i[\hat{H}, \hat{m}(r, t)]_- - \frac{1}{2}[\hat{W}(r), \hat{m}(r, t)]_+ \quad (2.1)$$

with the initial condition supposing that the RIPs are produced in a singlet state at a distance $r = r_0$

$$m_{SS}(r, 0) = \frac{\delta(r - r_0)}{4\pi r^2} \quad m_{ij}(r, 0) = 0 \text{ if } i \neq S \text{ or } j \neq S \quad (2.2)$$

with reflective boundary conditions at the contact distance $r = \sigma$

$$\left. \frac{\partial \hat{m}(r, t) e^{-r/\sigma}}{\partial r} \right|_{r=\sigma} = 0 \quad (2.3)$$

Here

$$\hat{L}_c = \frac{\tilde{D}}{r^2} \frac{\partial}{\partial r} r^2 e^{r/\sigma} \frac{\partial}{\partial r} e^{-r/\sigma} \quad (2.4)$$

is the encounter diffusion operator of the radical ions. \hat{H} is the spin Hamiltonian of the RIP, accounting for only the HFI with the donor electron spin

$$H = AIS_D \quad (2.5)$$

where A is the effective HFI constant, $I = 1/2$ is the spin of a nuclei, and $S_D = 1/2$ is the spin of the radical cation, D^+ . \hat{W} is the reaction operator of the RIP recombination

$$\hat{W}(r) = W_S(r) \hat{P}_S + W_T(r) \hat{P}_T \quad (2.6)$$

where \hat{P}_S and \hat{P}_T are the projection operators in the singlet and triplet states of the RIP, respectively. The notations of the commutator and anticommutator $[a, b]_{\pm} = ab \pm ba$ are used.

In this paper, the electron spin interaction with a number of nuclear spins is modeled by an interaction with a single nuclear spin with an effective HFI constant.²¹ In the system consisting of perylene/*N,N'*-dimethylaniline (Per/DMA), for both the anion radical and cation radical, all HFI constants are known.^{22,23} Estimations have shown the effective HFI constant of the radical cation DMA to be four times as great as that of the Per radical anion; therefore, the effective HFI constant of the RIP is mainly determined by the DMA radical. This is the reason why in eq 2.5 only the interaction between the donor and nuclear spins is held.

Equation 2.1 was solved in ref 16. The results for the quantum yields are given in terms of efficiencies, Z and Z_T

$$\varphi = \frac{\tilde{D}}{\tilde{D} + Z} \quad \varphi_T = \frac{Z_T}{\tilde{D} + Z} \quad \varphi_S = 1 - \varphi - \varphi_T \quad (2.7)$$

where

$$\frac{Z}{\tilde{D}} = z \frac{F/f}{1 + z(1 - F/f)} \quad \frac{Z_T}{\tilde{D}} = \frac{k_c^T k_c^S F - Z[1 + k_c^S(f - F)]/\tilde{D}}{k_c^S - k_c^T} \quad z = k_c^S f + (k_c^S - k_c^T) \cdot \frac{A}{B}$$

$$A = -6f[2 + (k_c^S + k_c^T)f]\{(1 + k_c^S f)[2 + (k_c^S + k_c^T)p]P + (k_c^S + k_c^T)qQ\} - [(1 + k_c^S p)(2 + (k_c^S + k_c^T)p) + k_c^S(k_c^S + k_c^T)q^2]F \quad (2.8)$$

$$B = 6f(k_c^S - k_c^T)[2 + (k_c^S + k_c^T)f]\{(2 + (k_c^S + k_c^T)p)P + (k_c^S + k_c^T)qQ\} - 2[8 + (3k_c^S + 5k_c^T)f]\{(2 + (k_c^S + k_c^T)p)^2 + (k_c^S + k_c^T)^2 q^2\}F \quad (2.9)$$

$$P = \text{Re } \tilde{G}_0(\sigma, r_0, iA) \quad Q = \text{Im } \tilde{G}_0(\sigma, r_0, iA) \quad F = \tilde{G}_0(\sigma, r_0, 0) \quad (2.10)$$

and

$$p = \text{Re } \tilde{G}_0(\sigma, \sigma, iA) \quad q = \text{Im } \tilde{G}_0(\sigma, \sigma, iA) \quad f = \tilde{G}_0(\sigma, \sigma, 0) \quad (2.11)$$

Here $\tilde{G}_0(r, r_0, s)$ is the Laplace transformation of the reaction-free Green function for continuous diffusion in the Coulomb potential obeying the equation

$$s \tilde{G}_0(r, r_0, s) = \hat{L}_c \tilde{G}_0(r, r_0, s) - \frac{\delta(r - r_0)}{4\pi r^2} \quad (2.12)$$

with the reflecting boundary conditions. The recombination is assumed to take place only in the vicinity of the contact, $\sigma \leq r \leq \sigma + \Delta$, where the layer width is very small, $\Delta \ll \sigma$. In the contact approximation, the recombination rates are determined by the equation

$$k_c^S = 4\pi\sigma^2\Delta \cdot W_S(\sigma) \quad k_c^T = 4\pi\sigma^2\Delta \cdot W_T(\sigma) \quad (2.13)$$

A close analytical approximation for the Green function, $\tilde{G}_0(\sigma, \sigma, s)$, was obtained in ref 24 and refined from misprints in ref 25. It takes the form

$$\tilde{G}_0(\sigma, \sigma, s) = \frac{1}{4\pi\tilde{D}\sigma} \cdot \frac{1}{\mu_0(\sigma) + \kappa(\sigma, s)} \quad (2.14)$$

where

$$\mu_0(\sigma) = \frac{1/x}{\exp(1/x) - 1} \quad \kappa(\sigma, s) = \frac{s\tau_d + [\nu(\sigma)/\varrho(\sigma)]\sqrt{s\tau_d}}{\sqrt{s\tau_d} + \nu(\sigma)} \quad \varrho(\sigma) = x^2 \exp(1/x) [1 - \exp(-1/x)]^2$$

and

$$\nu(\sigma) = \{x^3[\exp(1/x) + \exp(-1/x) - 2] - x\} \left\{ \frac{1}{6} [Ei(1/x) - \exp(1/x)(x + x^2 + 2x^3)] + \frac{1}{6} [E_1(1/x) - \exp(-1/x)(x - x^2 + 2x^3)] + \frac{2}{3}x^2 + x \right\}$$

$x = \sigma/r_c$, while Ei and E_1 are the integral exponential functions. At last, for the initial position, r_0 , close to the contact distance, the approximation can be used

$$\tilde{G}_0(\sigma, r_0, s) = \tilde{G}_0(\sigma, \sigma, s) \frac{1 - e^{-r_c/r_0}}{1 - e^{-r_c/\sigma}} \exp\{- (r_0 - \sigma)\sqrt{s/\tilde{D}}\} \quad (2.15)$$

In this equation, the action of the Coulomb potential on the motion between the initial position and the closest distance is neglected. Such an approximation is justified if the energy difference at these points is much less than the mean thermal energy $k_B T$. Therefore, eq 2.15 is applicable if the condition is met, $r_0 - \sigma \ll \sigma^2/r_c$.

III. Incoherent Spin Conversion Assistance of Double-Channel Geminate Recombination

The model of the incoherent spin conversion describes the recombination and separation of the geminate RIPs in terms of populations of RIP spin states. In this case, only diagonal elements of the density matrix are conserved, and the evolution equations are recast in the form²⁶

$$\frac{\partial m_S(r, t)}{\partial t} = \hat{L}_c m_S(r, t) + K_s m_T(r, t) - 3K_s m_S(r, t) - \frac{k_c^S}{4\pi\sigma^2} \delta(r - \sigma) m_S(r, t) \quad (3.1a)$$

$$\frac{\partial m_T(r, t)}{\partial t} = \hat{L}_c m_T(r, t) - K_s m_T(r, t) + 3K_s m_S(r, t) - \frac{k_c^T}{4\pi\sigma^2} \delta(r - \sigma) m_T(r, t) \quad (3.1b)$$

with the initial and boundary conditions determined by eqs 2.2 and 2.3. Here, $m_S = m_{SS}$ and $m_T = m_{T_0T_0} + m_{T_+T_+} + m_{T_-T_-}$ are the populations of the RIP's singlet and triplet states, respectively, and K_s is the phenomenological rate constant of the

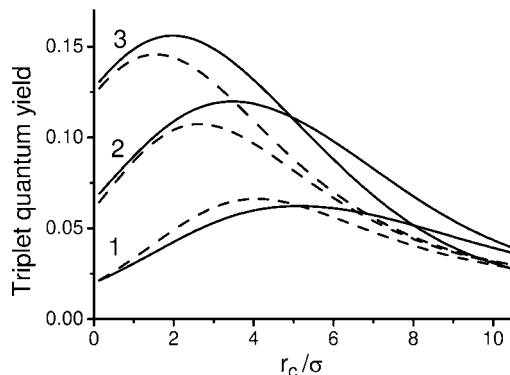


Figure 1. The triplet recombination quantum yield versus the Onsager radius, r_c , at different rates of the triplet charge recombination. The parameters are $\sigma = 7.5 \text{ \AA}$, $r_0 = 7.64 \text{ \AA}$, $k_c^S = 16800 \text{ \AA}^3/\text{ns}$, $\tilde{D} = 100 \text{ \AA}^2/\text{ns}$, $k_c^T = 2000 \text{ \AA}^3/\text{ns}$ (1), $k_c^T = 10000 \text{ \AA}^3/\text{ns}$ (2), $k_c^T = 77000 \text{ \AA}^3/\text{ns}$ (3), solid lines — coherent spin evolution, $A = 4.6 \text{ ns}^{-1}$, dashed lines — incoherent spin evolution, $K_s = A/32 = 0.143 \text{ ns}^{-1}$.

incoherent spin conversion. All of the rest of parameters are the same as those in the coherent model. For the contact recombination model, the solution for these equations determining the quantum yields in the limit $r_c \rightarrow 0$ was obtained in ref 13. This result can be easily generalized for interacting ion radicals.

In the general case, the recombination quantum yields can be represented in terms of the reaction-free Green function eq 2.12 as follows:

$$\varphi_T = 3k_c^T [(1 + k_c^S p_{\text{inc}})F - (1 + k_c^S f)P_{\text{inc}}] / \Delta \quad (3.2)$$

$$\varphi_S = k_c^S [(1 + k_c^T p_{\text{inc}})F + 3(1 + k_c^T f)P_{\text{inc}}] / \Delta \quad (3.3)$$

where

$$\Delta = 4 + (3k_c^S + k_c^T) p_{\text{inc}} + (k_c^S + 3k_c^T) f + 4k_c^S k_c^T p_{\text{inc}}$$

$P_{\text{inc}} = \tilde{G}_0(\sigma, r_0, 4K_s)$, $p_{\text{inc}} = \tilde{G}_0(\sigma, \sigma, 4K_s)$, f , and F are determined by eqs 2.10 and 2.11.

The discussion of the conditions of the incoherent model applicability as well as the comparative study of the coherent and incoherent approaches to systems of two interacting spin levels was carried out in ref 27.

When there is no Coulomb interaction, the coherent and incoherent models lead to very similar results for a wide area of parameters, provided the relationship is kept $A = 32K_s$.^{16,17} In the Coulomb well, however, there is an essential distinction between these models, as demonstrated in the next section.

IV. Results and Discussion

In Figures 1 and 2, the dependence of the triplet recombination quantum yield, φ_T , on the Onsager radius for several values of the triplet and singlet recombination rates is depicted. For comparison, the data are shown for the coherent (solid lines) and incoherent (dashed lines) models, correspondingly. The same parameters are exploited in both models, while $K_s = A/32$. These figures clearly demonstrate that an initial rise in the triplet quantum yield is inevitably followed by its decrease, except when the singlet recombination rate vanishes. In the last case (line 3 in Figure 2), the monotonous rise of φ_T up to unity is predicted. Such a behavior is the result of the interplay of two trends: the initial rise of the curves is conditioned by the extension of the RIP diffusional lifetime due to the Coulomb attraction of the ions, but in stronger fields, the proximity of the ion radicals results in an acceleration in the singlet

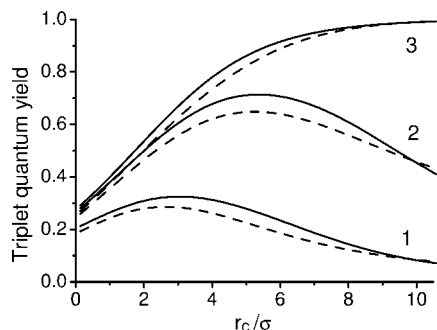


Figure 2. The triplet recombination quantum yield versus the Onsager radius, r_c , at different rates of the singlet charge recombination. The parameters are $\sigma = 7.5 \text{ \AA}$, $r_0 = 7.64 \text{ \AA}$, $k_c^T = 77000 \text{ \AA}^3/\text{ns}$, $\tilde{D} = 100 \text{ \AA}^2/\text{ns}$, $k_c^S = 5000 \text{ \AA}^3/\text{ns}$ (1), $k_c^T = 500 \text{ \AA}^3/\text{ns}$ (2), $k_c^S = 0$ (3), solid lines – coherent spin evolution, $A = 4.6 \text{ ns}^{-1}$, dashed lines – incoherent spin evolution, $K_S = 0.143 \text{ ns}^{-1}$.

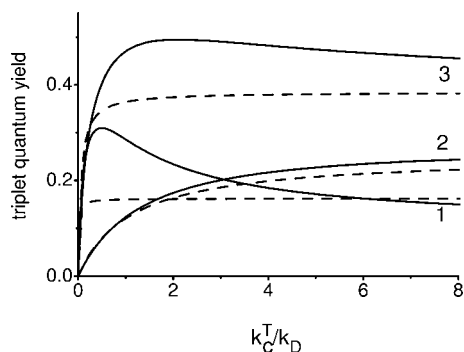


Figure 3. The triplet recombination quantum yield versus the triplet recombination rate constant, k_c^T . The parameters are $\sigma = 7.5 \text{ \AA}$, $r_0 = 7.64 \text{ \AA}$, $k_c^S = 2000 \text{ \AA}^3/\text{ns}$, $\tilde{D} = 100 \text{ \AA}^2/\text{ns}$, $r_c = 0$ (2), $r_c = 40 \text{ \AA}$ (3), $r_c = 80 \text{ \AA}$ (1), solid lines – coherent spin evolution, $A = 4.6 \text{ ns}^{-1}$, dashed lines – incoherent spin evolution, $K_S = 0.143 \text{ ns}^{-1}$.

recombination, so that the singlet-born pairs have no time for the singlet–triplet conversion. In weakly polar solvents, where the Coulomb potential is very strong, the singlet recombination dominates, and its quantum yield approaches unity, turning the yields of free ions and triplets to zero at $r_c \rightarrow \infty$. Of course, if the singlet recombination channel is closed, then the Coulomb attraction prolonging the pair's lifetime increases the triplet recombination and hinders their separation, so that the triplet quantum yield approaches unity in the same limit.

The dependencies of the quantum yields on the triplet recombination rate constant are depicted in Figure 3. As one might expect, φ_T increases with the triplet recombination rate constant, k_c^T . However, such a simple picture is observed only for relatively small values of the Onsager radius (line 2 in Figure 3). For stronger Coulomb potentials, the dependence of the triplet quantum yield on k_c^T becomes nonmonotonous. This nonmonotonous dependence is a distinctive property of the coherent spin evolution. Indeed, the model with incoherent spin transitions shows only a monotonous increase of φ_T with k_c^T (dashed lines in Figure 3). Such a behavior of quantum systems is well-known, in particular, in the magnetic resonance. It may be understood by the reference to a two-level system, with relaxation described by the Bloch equations that were used for the calculation of the radio field absorption. The latter appears to be small at either fast or slow relaxation, being maximal in between.²⁸ A RIP considered here executes the coherent spin transitions and, being in the triplet state, decays due to triplet recombination. In this process, there are two types of recombination impact on the spin system. The recombination results

in decay of both the diagonal and off-diagonal elements of the density matrix $\hat{m}(r, t)$. The decay of the diagonal elements (longitudinal relaxation) is nothing but the triplet recombination, whereas the off-diagonal element decay (transversal relaxation) suppresses the singlet–triplet transitions. When the triplet recombination rate is large enough, the singlet–triplet transitions become the narrow bottleneck on the path to the triplet neutral products. As a result, subsequent increase of k_c^T , suppressing the singlet–triplet transition rate, decreases the triplet quantum yield that we see in Figure 3.²⁹ A characteristic feature of this mechanism is the increase in the k_c^T value, at which the triplet quantum yield has a maximum, with A . In contrast, the incoherent model fully ignores the off-diagonal elements of the density matrix, and the mechanism of the singlet–triplet evolution suppression considered is absent. This results in a monotonous rise of φ_T with k_c^T .

To gain insight into which parameters determine whether the dependence of the triplet quantum yield on k_c^T is monotonous or nonmonotonous, let us consider a high polar solvent, $r_c \ll \sigma$, and the contact start, $r_0 = \sigma$. At this extreme, one can obtain a rather simple expression for the triplet quantum yield in the limit of a large triplet recombination rate, $k_c^T/k_d \gg 1$, k_c^S, θ

$$\varphi_T \approx \varphi_T^{(\infty)} \left\{ 1 + \frac{\varphi_T^{(\infty)}}{k_t} \left[2 + k_s - \frac{(1 + k_s)^2}{\theta} \right] \right\} \quad \varphi_T^{(\infty)} = \frac{\theta}{1 + k_s + \theta} \quad (4.1)$$

where $k_s = k_c^S/k_d$, $k_t = k_c^T/k_d$, $k_d = 4\pi\sigma\tilde{D}$ and

$$\theta = \frac{3}{8} \sqrt{\frac{A\sigma^2}{2\tilde{D}}} \quad (4.2)$$

The triplet quantum yield can approach its limiting value, $\varphi_T^{(\infty)}$, as $k_c^T \rightarrow \infty$, either from below or from above, depending on the sign of the expression in square brackets in eq 4.1. Apparently, the approaching from above implies that the function $\varphi_T(k_c^T)$ has a maximum. The maximum exists if the condition is fulfilled

$$\theta > \frac{(1 + k_s)^2}{2 + k_s} \quad (4.3)$$

When this inequality is reversed, a monotonous increase of φ_T with k_c^T is expected.

The difference between the value of φ_T in its maximum and $\varphi_T^{(\infty)}$, being very small in high polar solvents, strongly increases with r_c . The rise of r_c weakens the condition in eq 4.3, but nevertheless, the monotonous dependence of φ_T on k_c^T is realized in the area of small values of θ .

The question arises why the triplet recombination does not totally suppress the singlet–triplet transitions and why φ_T is finite at unlimited values of k_c^T . The reason is that the recombination events are separated by the time domains without recombination. The spin state of a RIP between two successive contacts can freely evolve, which results in a population of triplet states at any recombination rate. The Coulomb attraction shortening the time domains between contacts enhances the effectiveness of the off-diagonal matrix elements' suppression, leading to a more pronounced positive slope of φ_T .

The plots of the triplet quantum yield versus the HFI constant are pictured in Figure 4. This figure demonstrates a rather weak dependence of the free ion quantum yield on the HFI constant, although the difference between the singlet and triplet recombination rates is large enough. It is well-known that the dependence on A disappears in the case of equal rates $k_c^S = k_c^T$.¹

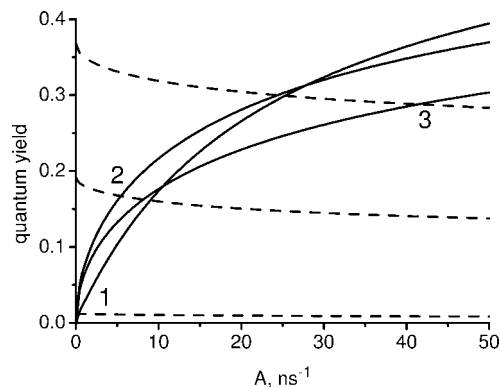


Figure 4. The triplet (solid lines) and free ion (dashed lines) quantum yields versus the HFI constant, A , at different values of the Onsager radius. The parameters are $\sigma = 7.5$ Å, $r_0 = 7.64$ Å, $k_c^S = 16800$ Å³/ns, $k_c^T = 77000$ Å³/ns, $\bar{D} = 100$ Å²/ns, $r_c = 0$ (3), $r_c = 12$ Å (2), and $r_c = 42$ Å (1).

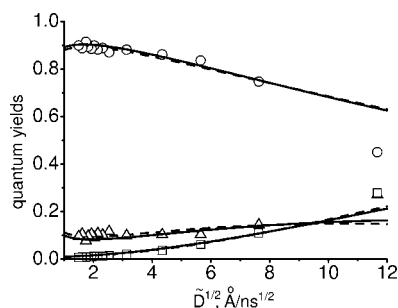


Figure 5. Fitting the theoretical quantum yields to the experimental data¹³ for singlet (○) and triplet (△) recombination, as well as charge separation (□). The parameters are solid lines — $r_c = 12$ Å, $A = 4.6$ ns⁻¹, $r_0 = 7.64$ Å, $k_c^S = 16800$ Å³/ns, $k_c^T = 77000$ Å³/ns; dashed lines — $r_c = 0$, $A = 47$ ns⁻¹, $r_0 = 7.54$ Å, $k_c^S = 48000$ Å³/ns, $k_c^T = 50000$ Å³/ns. The contact distance being an unadjustable parameter was set to $\sigma = 7.5$ Å.

Otherwise, this dependence is saturated as $A \rightarrow \infty$. For the parameters of interest in the particular system considered, the triplet quantum yield saturation is not achieved even for the HFI constant values as large as 50 ns⁻¹. The Coulomb interaction does not change the character of the triplet quantum yield dependence on the HFI constant, $\varphi_T \approx \gamma A^{1/2}$, in the area of small A but alters the proportionality coefficient. In the limits $r_c \ll \sigma$ and $\theta \ll 1$, one can obtain a simple equation for the triplet quantum yield

$$\varphi_T \approx \frac{k_t \theta}{(1 + k_s)(1 + k_c)} \quad (4.4)$$

In the Coulomb well, the coefficient, γ , is a rising function of r_c when it is not large but goes down with r_c in stronger fields.

Note that the singlet quantum yield monotonously rises and the free ion quantum yield monotonously goes down with the Onsager radius, r_c , so that these simple and obvious dependencies are not shown here.

V. Fitting the Contact Theories to the Experimental Data

The results of fitting the contact theories to the experimental data are displayed in Figure 5. They show that fittings of the same quality have been obtained in the framework of the approach accounting for the Coulomb interaction and without interaction. The most important difference between them is the value of the HFI constants obtained in the fittings. The inclusion of the Coulomb interaction, even in such a highly polar solvent

TABLE 1: The Variation of the Quantum Yields of the Triplet Recombination and the Charge Separation, With the Step-by-Step Modification of the Parameters between Those Obtained in the Fittings without and with the Coulomb Attraction^a

r_c , Å	k_c^S , Å ³ /ns	k_c^T , Å ³ /ns	A ns ⁻¹	φ_T	φ
0	48000	50000	47	0.152	0.163
12	48000	50000	47	0.190	0.080
12	48000	50000	4.6	0.073	0.080
12	16800	50000	4.6	0.151	0.173
12	16800	77000	4.6	0.155	0.169

^a The diffusion coefficient is set at $\bar{D} = 100$ Å²/ns.

as dimethyl sulfoxide–glycerol mixtures, with the static dielectric permittivity $\epsilon \approx 43$, decreases the HFI constant by a factor of 10. This value is rather unexpected because it is considerably larger than that obtained from the rough estimation of the encounter time (in the latter case, it is equal only to 2.5). Of course, that estimation was obtained under the supposition that all input parameters are kept unchangeable, except for the Onsager radius, but the fitting parameters have been considerably altered so that we cannot compare them. Nevertheless, such a large reduction of the HFI constant calls for elucidation.

To get an idea of how such a weak interaction (the energy of the Coulomb attraction at the smallest possible distance is less than $2k_B T$) can reduce the HFI constant by a factor of 10 in the fitting, we should take into account that the Coulomb attraction simultaneously retards the diffusional separation of RIPs and intensifies their recombination. The data listed in Table 1 show that the increase in the Onsager radius from 0 to 12 Å, with retention of the remaining parameters, strongly suppresses the free ion quantum yield and considerably raises φ_T . The reduction of the HFI constant from 47 to 4.6 ns⁻¹ strongly decreases φ_T , while φ is kept practically invariable. In the next step, a nearly three-fold reduction of the singlet recombination rate constant doubles both φ_T and φ , making them approach their initial values. The following increase of k_c^T from 50000 to 77000 Å³/ns does not improve the fitting at the point where $\bar{D} = 100$ Å²/ns but slightly improves it as a whole. It is worth noting that because of the weak sensitivity of the fitting to the triplet recombination rate magnitude, the uncertainty on k_c^T is large.

VI. Conclusions

The kinetics of single-channel recombination and separation of geminate RIPs are well-understood, and the theory often provides good fitting to the experimental data.^{14,26} The double-channel recombination assisted by spin conversion until recently has been much less studied, and the fitting is much less successful.¹⁷ The reason for this difference is as follows. In the single-channel case, there is a single variable parameter, the recombination rate. It turns out that this freedom provides the quantum yields needed and their dependence on the diffusion coefficient. In the double-channel case, both of the recombination rate constants (to singlet and triplet products) are considered to be adjustable. When the parameters controlling the spin conversion were also adjustable, excellent fitting to the theory was obtained.^{15,17} The mechanism of the spin conversion was firmly established⁷ and the effective HFI constant was determined in independent experiments. When the HFI constant is stated, the theory becomes much less flexible. In such a situation, the fitting requires more adequate models, and its results become more reliable. In particular, the investigation of the double-channel recombination performed in this paper states that the Coulomb interaction plays an important role in the fate of

geminate RIPs. The reliable fitting is impossible if it is not properly accounted for. Of course, we realize that the model explored in this paper, which treats the polar solvent in terms of a macroscopic dielectric permittivity without space dispersion and where the radical ions are considered to be spheres, may be insufficient for a quantitative description of the geminate RIP's recombination and separation kinetics.

For the past few years, several different approaches have been developed to fit the experimental data on the double-channel recombination of geminate RIPs.^{13,15,17} Now, we can systematize the results, including those obtained in this paper. Applying the contact approximation and coherent HFI mechanism of the spin conversion, we have found from the best fit the value of the HFI constant in the absence of the Coulomb interaction, $A = 47 \text{ ns}^{-1}$. For the incoherent model, the spin conversion rate $K_s = 1.5 \text{ ns}^{-1} \approx A/32$ was earlier obtained in the contact approximation.¹³ Using the exponential dependence on the ion separation for both the ionization and recombination rates, a noticeably smaller value of $K_s = 0.75 \text{ ns}^{-1}$ was obtained from the fitting.¹⁵ Hence, the remote character of the ionization and recombination decreases the spin conversion constant needed for the fitting. Assuming both ionization and recombination are carried out by the Marcus electron-transfer rates, the value $A = 9 \text{ ns}^{-1}$ was obtained,¹⁷ which is more than 5 times smaller than that found from the fitting to the contact model. If we suppose that the Coulomb attraction decreases the HFI constant for remote ionization and recombination as much as at the contact recombination, then we obtain for the latter case a 10 times smaller $A = 0.9 \text{ ns}^{-1}$. This value does not differ so dramatically from that obtained experimentally for DMA^+ and Per^- , which is equal to $A = 0.4 \text{ ns}^{-1} = 23 \times 10^{-4} \text{ T}$.¹⁷ Moreover, it is well-known that lowering the screening at short distances decreases the dielectric permittivity, which considerably strengthens the Coulomb attraction between counterions.³⁰ This may result in even a more profound decrease of the HFI constant. However, the effect of spatial dispersion, as well as remote ionization and recombination, may be investigated by numerical methods only. We plan to perform such an exploration in the near future.

Acknowledgment. A.I.I. gratefully acknowledges the Weizmann Institute of Science for hospitality during his stay in Israel

and the Russian Foundation for Basic Researches, Grant No. 07-03-96600.

References and Notes

- (1) Schulten, K.; Staerk, H.; Weller, A.; Werner, H.-J.; Nickel, B. Z. *Phys. Chem. (Frankfurt/Main)* **1976**, *101*, 371.
- (2) Schulten, Z.; Schulten, K. *J. Chem. Phys.* **1977**, *66*, 4616.
- (3) Weller, A.; Staerk, H.; Treichel, R. *Faraday Discuss. Chem. Soc.* **1984**, *78*, 271.
- (4) Ottolenghi, M. *Acc. Chem. Res.* **1973**, *6*, 153.
- (5) Michel-Beyerle, M. E.; Haberkorn, R.; Bube, W.; Steffens, E.; Schröder, H.; Neusser, H. J.; Schlag, E. W. *Chem. Phys.* **1976**, *17*, 139.
- (6) Brocklehurst, B. *Chem. Phys. Lett.* **1974**, *28*, 357.
- (7) Werner, H.-J.; Staerk, H.; Weller, A. *J. Chem. Phys.* **1978**, *68*, 2419.
- (8) Steiner, U. E.; Ulrich, Th. *Chem. Rev.* **1989**, *89*, 51.
- (9) Weller, A.; Nolting, F.; Staerk, H. *Chem. Phys. Lett.* **1983**, *96*, 24.
- (10) Roest, M. R.; Oliver, A. M.; Paddon-Row, M. N.; Verhoeven, J. W. *J. Phys. Chem. A* **1997**, *101*, 4867.
- (11) Neufeld, A. A.; Burshtein, A. I.; Angulo, G.; Grampp, G. *J. Chem. Phys.* **2002**, *116*, 2472.
- (12) Angulo, G.; Grampp, G.; Neufeld, A. A.; Burshtein, A. I. *J. Phys. Chem. A* **2003**, *107*, 6913.
- (13) Gladkikh, V. S.; Burshtein, A. I.; Angulo, G.; Grampp, G. *Phys. Chem. Chem. Phys.* **2003**, *5*, 2581.
- (14) Burshtein, A. I. *Adv. Chem. Phys.* **2004**, *129*, 105.
- (15) Gladkikh, V. S.; Angulo, G.; Burshtein, A. I. *J. Phys. Chem. A* **2007**, *111*, 3458.
- (16) Lukzen, N. N.; Pedersen, J. B.; Burshtein, A. I. *J. Phys. Chem. A* **2005**, *109*, 11914.
- (17) Dodin, D. V.; Ivanov, A. I.; Burshtein, A. I. *J. Phys. Chem. A* **2008**, *112*, 889.
- (18) Salikhov, K. M.; Molin, Yu. N.; Sagdeev, R. Z.; Buchachenko, A. L. *Spin Polarization and Magnetic Effects in Radical Reactions*; Akademian Kiado: Budapest, Hungary and Elsevier: Amsterdam, The Netherlands, 1984.
- (19) Korst, N. N.; Lazarev, A. V. *Physica* **1969**, *42*, 31.
- (20) Pedersen, J. B.; Freed, J. H. *J. Chem. Phys.* **1973**, *58*, 2746.
- (21) Salikhov, K. M. *Chem. Phys.* **1983**, *82*, 145.
- (22) Pobedimskii, B. G.; Buchachenko, A. L.; Neiman, M. B. *Russ. J. Phys. Chem.* **1968**, *42*, 129.
- (23) Möbius, K. Z. *Naturforsch., A: Phys. Sci.* **1965**, *20*, 1102.
- (24) Zharikov, A. A.; Shokhirev, N. V. *Chem. Phys. Lett.* **1992**, *186*, 253.
- (25) Zharikov, A. A.; Shokhirev, N. V. *Z. Phys. Chem.* **1992**, *177*, 37.
- (26) Burshtein, A. I. *Adv. Chem. Phys.* **2000**, *114*, 419.
- (27) Burshtein, A. I. *Chem. Phys. Lett.* **2005**, *411*, 66.
- (28) Abragam, A. *The Principles of Nuclear Magnetism*; Clarendon Press: Oxford, U.K., 1961.
- (29) The singlet recombination also suppresses the singlet-triplet transitions leading to the decay of the density matrix off-diagonal elements. In this case, the decay of both the diagonal and off-diagonal elements results in a decrease of the triplet quantum yield. This behavior may be seen in Figure 2.
- (30) Kornyshev, A. A.; Ulstrup, J. *Chem. Phys. Lett.* **1986**, *126*, 74.

JP800008N